Alignment and Morphology Control of Ordered Mesoporous Silicas in Anodic Aluminum Oxide Channels by Electrophoretic Deposition

Justin J. Hill,[†] Sonja P. Cotton,[†] and Kirk J. Ziegler*[,†,‡,§]

Department of Chemical Engineering, Department of Materials Science and Engineering, and Center for Surface Science and Engineering, University of Florida, Gainesville, Florida 32611

Received November 12, 2008. Revised Manuscript Received March 10, 2009

Reproducible alignment and complete inclusion of ordered mesoporous structures into anodic aluminum oxide (AAO) is still a challenging nanofabrication process. Hierarchical nanostructures of ordered mesoporous silica (OMS) in AAO channels were prepared directly on conducting substrates by electrophoretic deposition of colloidal silica nanoparticles in sols containing a structure directing agent. The mesoporous silica structures were found to be highly dependent on the magnitude of the applied electric field and moderately dependent on the overall deposition time. At low applied voltages, disordered porous tubules are formed. At an applied voltage of 5 V and deposition times in excess of 7 h, ordered mesoporous silicas fill the AAO channels, and the OMS pores display the onset of axial alignment with respect to the AAO pore. The deposition of the mesoporous silica structures with preferential axial alignment on conductive supports is described by a new self-assembly mechanism based on selective solvent exclusion due to confined particle packing of colloidal silica.

Introduction

The fabrication of nanostructures with large aspect ratios and diameters below 10 nm is a rapidly emerging area of interest in many fields of engineering and science. For example, the assembly of conducting, semiconducting, magnetic, and photonic materials via ordered porous templates is an attractive means of producing two-dimensional arrays of nanorods.[1−8] AAO films,[9,10] polycarbonate track etched membranes,[11] block copolymers,[12] and nanochannel glasses[4] have been successfully used for the templated growth of nanorods. However, the preparation of templates that can simultaneously control diameter, length, and orientation remains a challenge. To achieve long-range orientation control with nanorod dimensions where finite size effects become important, new porous template processes may be needed, especially for direct fabrication on substrates or functional devices. These ordered architectures might facilitate "bottom-up" alternatives to conventional lithographic techniques.

Both mesoporous silicas and porous alumina have been widely used for the template-based fabrication of nanorods.[13] The unidirectional channels of AAO provide an excellent architecture for template-based patterning of nanostructures and devices. While these templates are useful in preparing ordered arrays of pores with diameters between 20 and 200 nm, the channel dimensions are often too large to engineer nanorods that exhibit quantum confinement effects. On the other hand, mesoporous materials have hexagonal-packed pores with uniform diameters between 2 and 15 nm.[14,15] Mesoporous silica is fabricated by the condensation of colloidal silica nanoparticles in the presence of a self-assembling structure directing agent (SDA). As a result of the local molecular environment (e.g., hydrophilicity, steric, and van der Waals energetics), the SDA molecules will self-assemble into thermodynamically stable mesopores. On a nanometer scale, self-assembled SDA structures can be highly ordered—providing a self-assembled porous structure

* Corresponding author. E-mail: kziegler@che.ufl.edu.
[†] Department of Chemical Engineering.
[‡] Department of Materials Science and Engineering.
[§] Center for Surface Science and Engineering.

(1) Cao, G. Z. *J. Phys. Chem. B* **2004**, *108* (52), 19921–19931.
(2) Chu, S. Z.; Inoue, S.; Wada, K.; Li, D.; Haneda, H.; Awatsu, S. *J. Phys. Chem. B* **2003**, *107* (27), 6586–6589.
(3) Hussen, G.; Shirakawa, H.; Nix, W.; Clemens, B. *J. Appl. Phys.* **2006**, *100*, 114322.
(4) Limmer, S. J.; Seraji, S.; Wu, Y.; Chou, T. P.; Nguyen, C.; Cao, G. Z. *Adv. Funct. Mater.* **2002**, *1* (12), 59–64.
(5) Cott, D. J.; Petkov, N.; Morris, M. A.; Platschek, B.; Bein, T.; Holmes, J. D. *J. Am. Chem. Soc.* **2006**, *128* (12), 3920–3921.
(6) Chung, Y.; Lee, C.; Peng, C.; Chiu, H. *Mater. Chem. Phys.* **2006**, *100*, 380–384.
(7) Zhang, Q.; Li, Y.; Xu, D.; Gu, Z. *J. Mater. Sci. Lett.* **2001**, *20*, 925–927.
(8) Petkov, N.; Platschek, B.; Morris, M. A.; Holmes, J. D.; Bein, T. *Chem. Mater.* **2007**, *19* (6), 1376–1381.
(9) Li, Y.; Xu, D.; Zhang, Q.; Chen, D.; Huang, F.; Xu, Y.; Guo, G.; Gu, Z. *Chem. Mater.* **1999**, *11*, 3433.
(10) Schmid, G.; Baumle, M.; Geerkens, M.; Heim, I.; Osemann, C.; Sawitowski, T. *Chem. Soc. Rev.* **1999**, *28*, 179.
(11) Schonenberger, C.; van der Zande, B. M. I.; Fokkink, L. G. J.; Henny, M.; Schmid, C.; Kruger, M.; Bachtold, A.; Huber, R.; Staufer, U. *J. Phys. Chem. B* **1997**, *101*, 5497.
(12) Zschech, D.; Kim, D. H.; Milenin, A. P.; Scholz, R.; Hillebrand, R.; Hawker, C. J.; Russell, T. P.; Steinhart, M.; Gosele, U. *Nano Lett.* **2007**, *6* (7), 1516–1520.
(13) Xia, Y.; Yang, P.; Sun, Y.; Wu, Y.; Mayers, B.; Gates, B.; Yin, Y.; Kim, F.; Yan, H. *Adv. Mater.* **2003**, *15* (5), 353–389.
(14) Ciesla, U.; Schuth, F. *Microporous Mesoporous Mater.* **1999**, *27*, 131.
(15) Schuth, F. *Chem. Mater.* **2001**, *13*, 3184.
(16) Ryan, K. M.; Coleman, N. R. B.; Lyons, D. M.; Hanrahan, J. P.; Spalding, T. R.; Morris, M. A.; Steytler, D. C.; Heenan, R. K.; Holmes, J. D. *Langmuir* **2002**, *18* (12), 4996–5001.
(17) Hanrahan, J. P.; Copley, M. P.; Ziegler, K. J.; Spalding, T. R.; Morris, M. A.; Steytler, D. C.; Heenan, R. K.; Schweins, R.; Holmes, J. D. *Langmuir* **2005**, *21*, 4163.

10.1021/cm803083s CCC: $40.75
Published on Web 04/10/2009

with diameters that can be tuned by changing the surfactant[16] or swelling the micelle core.[17]

On a bulk scale, ordered mesoporous silicas have randomly oriented pore axes. Researchers have attempted to prepare vertically oriented mesoporous membranes on substrates. However, these substrates have yet to display long-range pore ordering, instead yielding domains of pores with different orientation.[17−19] Further benefits of mesoporous materials could be realized if the pore domains could be preferentially aligned into long-range ordered porous substrates.

Researchers have recently used the channels of AAO membranes as templates for preparing OMS domains inside the alumina membrane.[5,8,20,21] The general method to construct hierarchical OMS/AAO membranes is to carefully force the mesoporous silica sol through the channels of the AAO template. The OMS sol is forced through the AAO channels by either dipping and then withdrawing the AAO template from the sol, drop-coating the sol directly onto the AAO template, or drawing the precursor solution through the AAO template by a pressure differential.[5,20−22] In these methods, OMS structures are formed by self-assembly due to precursor evaporation within the AAO pore.

These hierarchical OMS/AAO structures demonstrate the ability to combine these two porous systems but remain far from idealized structures that are reproducible. Evaporative-induced self-assembly results in OMS structures within the AAO channels, but in most cases only a small fraction of each AAO channel is filled with mesoporous silica. These voids in the OMS structure are formed because of OMS sol condensation, which expand further during calcination. These voids in the OMS/AAO hierarchical structure minimize their effectiveness in nanofabrication. In addition, the OMS structures often have multiple ordered phases (e.g., axial, circular, helical) with a small fraction oriented in the preferred axial direction.[5,8,20,21] The ideal OMS/AAO hierarchical structure would have high inclusion of OMS within AAO channels where all OMS pores are uniform in diameter and axially aligned along the AAO channel.

Additional forces during inclusion can also help orient the OMS structure within the AAO pore. Teramae and co-workers demonstrated a high degree of axially aligned pores of uncalcined OMS in AAO by pulling the sol through the AAO channels with a vacuum.[22] The additional shear force may help axially orient the pores. Researchers have also shown that ionic and nonionic SDAs as well as colloidal silica will align with respect to an applied electric field.[23,24] Trau and co-workers used this alignment as well as electro-osmotic flow and joule heating to fabricate highly ordered OMS with high aspect ratios in PMMA microchannels.[25] While this method fabricated aligned OMS that completely filled the open channels, the large electric fields caused extensive hydrolysis (vigorous bubbling) at the electrodes. This hydrolysis would destroy the structure and ordering of the mesoporous silica fabricated directly on substrates, such as the OMS grown from the electrode upward through the AAO channel in this study. Further, the closure of one end of the AAO channel hinders transport of the sol into the pores. In this paper, ordered mesoporous silicas are fabricated directly onto conductive supports within AAO channels using moderate electric fields to minimize hydrolysis. Electrophoretic deposition of colloidal silica in a nonionic SDA sol facilitates the construction of hierarchical OMS/AAO membranes on conductive supports with mesoporous structures that are highly dependent on the applied electric field and deposition time. At high potentials and long deposition times, the OMS shows the onset of axial alignment.

Experimental Section

Precursor Solutions. The mesoporous silica sol for dip-coating and electrophoretic deposition were prepared via a two-step synthesis procedure previously reported by Holmes and co-workers.[15] At room temperature, water, ethanol, tetraethyl orthosilicate (TEOS), and 0.2 M HCl were mixed so that the mass ratio was 1:2.19:1.16:1.67. The solution was then placed in a rotoevaporator and held at 60 °C for 1 h to facilitate the acid-catalyzed hydrolysis−condensation of the colloidal silica. In another beaker, poly(ethylene oxide)-*b*-poly(propylene oxide)-*b*-poly(ethylene oxide) triblock copolymer, Pluronic 123 (P123), was dissolved in ethanol by mechanical stirring for 1−2 h to obtain a 5 wt % (approx.) solution. These two solutions were then combined and mixed for 2 h in a sealed beaker to obtain a clear, low viscosity, isotropic suspension of colloidal P123/silica particles.

Precursor Electrophoretic Deposition. Whatman AAO membranes with an average pore diameter of 200 nm were mounted on an aluminum electrode with lead foil and placed in the room temperature sol opposite a lead counter electrode; the two electrodes were approximately 10 cm apart. Since the solution pH was below 2 and thus below the isoelectric point of silica, cathodic deposition of the silica occurs. The electrodes were connected to a DC power supply (Lambda Gen300-5), and the voltage was increased slowly at a rate of 0.1 V/s. The electrophoretic deposition was carried out at potentials of 0.3, 2.3, and 5 V and times between 3 and 18 h. After OMS deposition, the membranes were air-dried for 2 h while still mounted to the aluminum electrode. The templates were subsequently removed from the electrode and calcined in air for 4 h in a muffle furnace (Barnstead Thermolyne 30400) at 450 °C using a ramp rate of 1−2 °C/min.

Characterization. The samples were characterized by X-ray diffraction (XRD) (Philips MRD X'Pert System) and high-resolution transmission electron microscopy (HRTEM) (JEOL FETEM 2010F). For XRD analysis, the entire OMS/AAO substrate was ground into a powder and attached to a glass slide with double-sided tape. After aligning the sample with respect to the X-ray beam, scans were recorded from 0 to 10° 2θ. HRTEM samples were prepared by dissolving the alumina membrane with 25 wt % phosphoric acid for several hours, diluting with DI water, and drop

(18) Miyata, H.; Kuroda, K. *J. Am. Chem. Soc.* **1999**, *121*, 7618–7624.
(19) Miyata, H.; Suzuki, T.; Fukuoka, A.; Sawada, T.; Watanabe, M.; Noma, T.; Takada, K.; Mukaide, T.; Kuroda, K. *Nat. Mater.* **2004**, *3* (9), 651–656.
(20) Wu, Y.; Cheng, G.; Katsov, K.; Sides, S. W.; Wang, J.; Tang, J.; Fredrickson, G. H.; Moskovits, M.; Stucky, G. D. *Nat. Mater.* **2004**, *3* (11), 816−822.
(21) Yoo, S. J.; Ford, D. M.; Shantz, D. F. *Langmuir* **2006**, *22* (4), 1839–1845.
(22) Yamaguchi, A.; Uejo, F.; Yoda, T.; Uchida, T.; Tanamura, Y.; Yamashita, T.; Teramae, N. *Nat. Mater.* **2004**, *3*, 337–341.
(23) Liang, K. M.; Huang, W. L.; Gu, S. R. *Mater. Res. Bull.* **2000**, *35*, 115–123.
(24) Tsori, Y.; Tournilhac, F.; Andelman, D.; Leibler, L. *Phys. Rev. Lett.* **2003**, *90* (14), 145504(1)–145504(4).
(25) Trau, M.; Yao, N.; Kim, E.; Xia, Y.; Whitesides, G. M.; Aksay, I. A. *Nature (London)* **1997**, *390* (6661), 674–676.

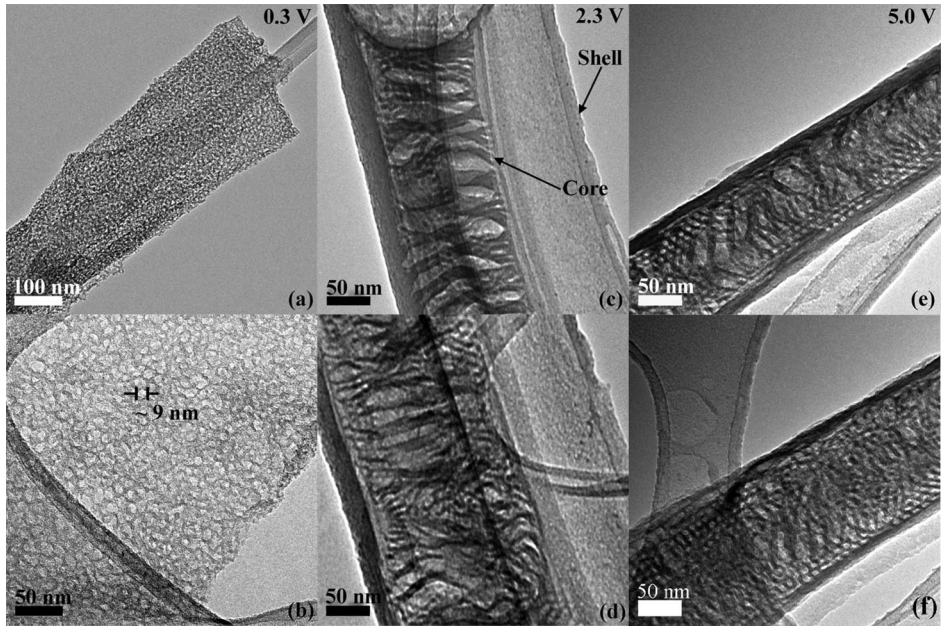

Figure 1. HRTEM of a typical OMS hierarchical nanostructure obtained from the electrophoretic deposition of a mesoporous silica precursor for 3 h within a 200 nm pore diameter AAO template at (a, b) 0.3 V, (c, d) 2.3 V, and (e, f) 5 V, respectively. The morphology changes from nanotubule structures at low voltages (a, b) to ordered mesoporous structures at higher voltages (e, f).

coating the solution onto a Lacey Carbon TEM grid. HRTEM images were taken using an accelerating voltage of 200 kV.

Results

Colloidal silica particles are known to have a net positive surface charge in solutions with a pH below 2. This surface charge provides the primary driving force for particle movement in applied electric fields, enabling the electrophoretic deposition of many oxides, including SiO_2.[23] Figure 1 depicts HRTEM images of silica nanorods liberated from the OMS/AAO hierarchical structures after electrophoretic deposition at various voltages and a deposition time of 3 h (see Supporting Information for more TEM images). An important distinction of these nanostructures from previous work is that the diameter of the nanostructures after calcination (~200 nm) are similar to the AAO channels (~200 nm) and independent of applied voltage. However, the applied electric field strongly affects the nanostructure morphology. As the applied electric field is increased, the structures shift from nanotubules to more completely filled nanorods. At the applied voltage of 0.3 V shown in Figure 1a,b, a nanotubule structure is formed with disordered mesopores (diameters ~ 9 nm) along the entire length of the structure. At the higher voltages (2.3 V) shown in Figure 1c,d, the same mesoporous shell is formed on the pore wall as well as an internal (core) mesoporous structure. As seen in Figure 1d, a significant void remains, and the core structure is composed of a disordered mesoporous structure. Ordered pore orientations become apparent when a bias of 5 V is applied as seen in Figure 1e,f. In addition to this ordering at high potentials, the core structure fills more of the AAO channel. The diameters of the individual mesopores in the nanorod core are approximately 10 nm.

The OMS/AAO hierarchical structures formed at 5 V and 3 h of electrophoretic deposition time can show helical ordering, such as that shown in Figure 1f or axial ordering. For example, Figure 2a shows a nanorod liberated from the AAO template, which shows both mild radial ordering and the beginnings of axial ordering. It was observed that axially oriented pores were most prominent at the nanorod end near the substrate, suggesting that the electric field affected the ordering of the pores.

Deposition time strongly affects the nanorod length as expected (not shown) but also introduces more orientation changes. At deposition times longer than 7 h, the electric field appears to introduce preferential axial alignment of the pores within the AAO channel as shown in Figure 2b. This axial ordering is especially evident in the inset. The nanorods are also more uniformly filled and lack the coaxial structure observed at shorter deposition times. While electrophoretic deposition at 3 h only showed 9% of the nanorods with some amount of axial alignment, 92% of the nanorods deposited for 7−8 h showed the onset of axial alignment (see Supporting Information). Therefore, it appears that axially aligned pores begin to form after 3 h and continue to evolve during electrophoretic deposition. Figure 3 helps illustrate the morphological changes observed along the length of a nanorod deposited at 5 V for 7 h. Near the electrode, the nanorod appears to be completely filled, and the mesopores are oriented axially (Figure 3d). At sections further away from the electrode, the nanorod is not completely filled, and the axial alignment is replaced by a helical alignment (Figure 3c). Moving further away from the electrode, some mesoporous ordering is still present (Figure 3b); however, a majority of the structure is disordered silica. This section appears similar to the nanorods obtained at 5 V and 3 h of electrophoretic deposition (Figure 1e and Supporting Information Figure S3). At the end of the deposited nanorod, the nanorod tapers into a thin shell similar to what is observed

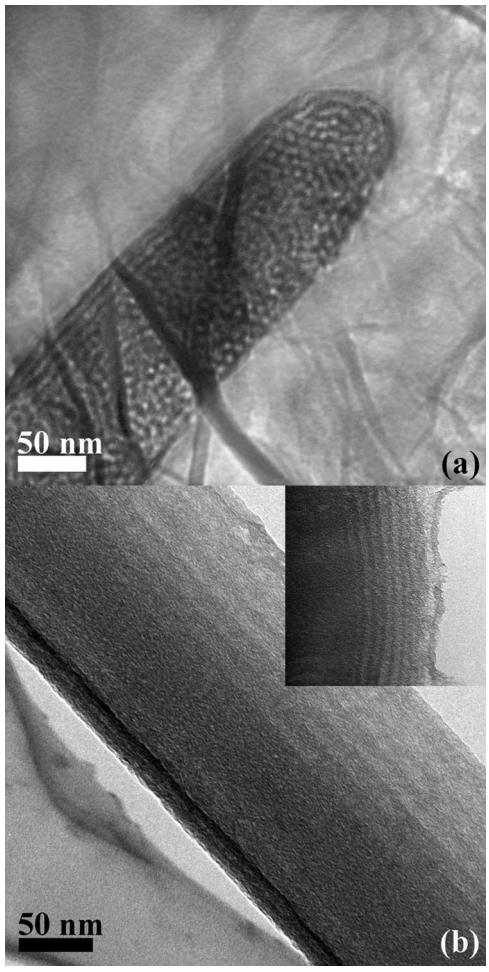

Figure 2. Effect of deposition time on OMS axial ordering. HRTEM of a typical OMS hierarchical nanostructure obtained from the electrophoretic deposition of a mesoporous silica precursor within a 200 nm pore diameter AAO template at 5 V for (a) 3 h and (b) 8 h. The inset highlights the axial ordering seen after long deposition times. Only the mesopores near the edge of the nanorod are visible as a result of limited electron transmission at the center/thicker areas of the nanorod.

at low deposition voltages (see Figure 1a,b and Supporting Information Figure S1). Notice that some axial alignment near the edges can persist to the end of the nanorod.

Further indication of mesoporous ordering can be found in the XRD data found in Figure 4. The spectra at 5 V and 8 h of mesoporous silica electrophoretic deposition in Figure 4 clearly shows a reflection corresponding to the mesopore lattice. The *d*-spacing of this peak corresponds to a distance of approximately 13 nm. If hexagonally close packed (HCP) ordering is assumed, the expected mesopore center-to-center distance is 15 nm. From the HRTEM images in Figures 1f, 2, and 3, the center-to-center distance between pores is approximately 15 nm, and thus the pore diameter is approximately 10 nm. These dimensions are within the range of diameters obtained by other researchers.[8,16,20]

Discussion

It is apparent that the electric field is important in determining the structure of the nanorods and the mesopore orientation within the AAO channels. The transition region observed near the end of the electrodeposited nanorod (see Figure 3a and Supporting Information Figure S1) is interesting. On the basis of data presented by Okubo,[26] the average diameter of the colloidal silica particles is less than 10 nm. If the colloidal particles have diameters between 1 and 10 nm, the sol would have a concentration on the order of $10^{14}-10^{17}$ nanoparticles/mL. Assuming thermal equilibrium and no surface charging effects from the alumina, it is estimated that each AAO channel has approximately 500 to 500 000 nanoparticles. This small number of particles is insufficient to completely fill the channel but could thinly coat the channel walls. Therefore, the thin shells observed in Figure 1a,b and the ends of the nanorods in Figure 3a and Supporting Information Figure S1 are likely formed by residual colloidal particles remaining in the AAO channel after the electric field was turned off. The bulk of the nanorod must then be deposited by an electrophoretic mechanism that drives colloidal particles to the electrode.

To further probe the mechanism of OMS formation in the presence of an electric field, nanorods were prepared by dip-coating the membranes (attached to substrate) in the sol (i.e., no applied voltage). HRTEM images of the nanorods formed inside the AAO channel in Figure 5 clearly show an amorphous silica nanotubule structure similar to those obtained using electrophoretic deposition at 0.3 V. The lack of any ordered structure was also confirmed by the XRD data in Figure 4. The dip-coated nanotubules observed in Figure 5 differ from previous work.[5,8,20,21] Although our sol composition differed slightly from prior work, the most significant difference is the conductive backing. Most prior approaches benefited from the forced flow of solution through the channel. As a layer of silica is deposited, the forced flow introduces additional silica, which can deposit due to shear-induced aggregation. An exception is the OMS structures obtained by Stucky and co-workers with one AAO pore end closed.[20] However, the colloidal silica and P123 concentrations were much higher, allowing more particles to enter each AAO channel. At the low precursor concentrations used in this study, only a minor flux of nanoparticles enter the channel without forced flow. The low concentration of particles in the channel is insufficient to obtain OMS hierarchical structures. However, the alumina surface will have a net negative charge at the solution pH, leading to a Coulombic attraction of the positively charged silica nanoparticles and a tubular structure.

The evaporation-induced self-assembly processes can be understood by analyzing the ternary phase diagram in Figure 6 for a mixture of water, ethanol, and P123 modified from experimental data.[27] Although the phase diagram shown in Figure 6 does not account for potential interactions with the AAO template, it can be used to illustrate the observed morphological changes. Sols used in this work or by others [5,8,20,21] begin in the "ethanol rich" region of the phase diagram (e.g., point A in Figure 6). In this region, no micelles exist, and the solution is an isotropic colloidal suspension. To obtain an HCP (hexagonal close packed) arrangement of rod-like micelles, the solution must drop from the ethanol

(26) Okubo, T. *J. Colloid Interface Sci.* **1988**, *125* (2), 380–385.
(27) Soni, S. S.; Brotons, G.; Bellour, M.; Narayanan, T.; Gibaud, A. *J. Phys. Chem. B* **2006**, *110*, 15157–15165.

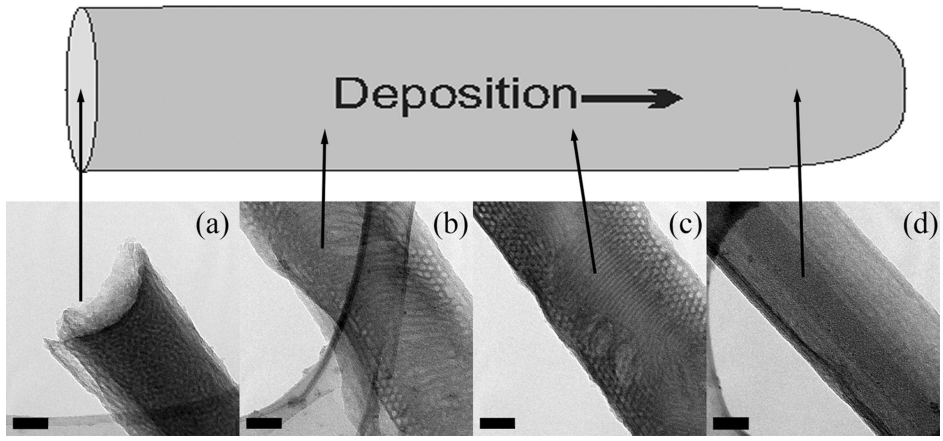

Figure 3. Stages of axial mesopore formation. (a−d) Progressive HRTEM images along the length of a nanorod electrophoretically deposited at 5 V for 7 h. Image (d) is taken at the end of the nanorod closest to the electrode, where axial ordering is fully developed. Further away from the electrode, the (c) nanorod still shows ordered mesopores but is helically rather than axially aligned. These mesopores become disordered further away in image (b). Finally, only slight axial ordering is observed near the edges with a majority of the nanorod having disordered mesopores as seen in image (a). All scale bars are 50 nm.

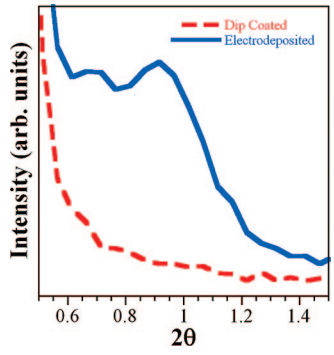

Figure 4. XRD data from OMS electrodeposited in 200 nm pore diameter AAO at 5 V and that of a similar AAO template with a conductive backing dipped in an identical solution. All deposition times were 8 h. Electrophoretically deposited nanostructures depict a characteristic lattice reflection, whereas the dip-coated sample does not.

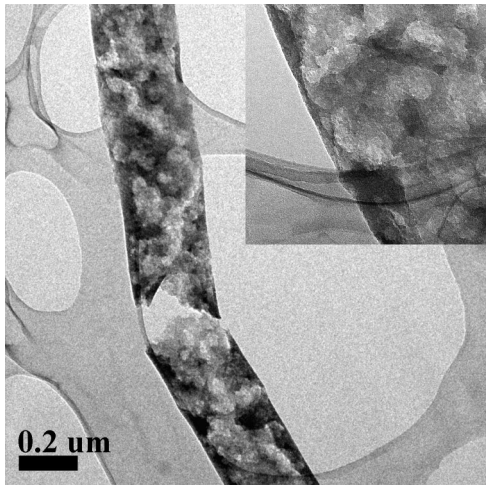

Figure 5. HRTEM of a typical silica nanotubule obtained from dip-coating a 200 nm pore diameter AAO template with a mesoporous silica precursor for 8 h. Although these dip-coated samples have similar structures to the electrophoretically deposited nanotubules at low voltages, these samples do not have the mesoporous walls seen in Figure 1a,b.

rich region to the region marked as HCP. This region is composed of roughly 1:1 ratios of water and P123, with a small amount of ethanol present. Once the AAO template is removed from the OMS precursor solution, the system is at point B. At this point in the evaporative-induced self-assembly, the sol within the AAO pore contains a higher concentration of colloidal particles but is still isotropic. Ethanol then evaporates, moving the system toward point C (just outside the isotropic−HCP boundary). HCP OMS then begins to form spontaneously as the solution within the AAO channel continues to evaporate, leaving the resulting OMS somewhere between point D and point E depending on channel size and shape, evaporation kinetics, and other parameters. Further removal of ethanol and water during calcination results in significant shrinkage of the OMS structures obtained.[5,8,20,21]

An immediate difference in the structure of the nanorods was apparent when the deposition was carried out by an applied electric field. Interestingly, the presence of even a small electric field has an important effect on the morphology, yielding porous nanotubules as shown in Figure 1a,b. Further, the channels are completely filled and show axial alignment at long deposition times. These results suggest that OMS formation occurs by a different mechanism. Application of a DC field causes the particles to flow into the AAO channels toward the electrode and to pack the nanoparticles closer together. If the silica particles are not only hydrated but also coated with P123, the electric field packing would selectively exclude ethanol, dropping the local solution closer to the HCP region (point C). Joule heating may also have a role in the removal of ethanol. Higher voltage potentials draw more particles into the AAO channel and push the system into the HCP region of the ternary phase diagram (point D in Figure 6). Although this process should yield a random orientation of the OMS, it appears that the electric field (oriented parallel to the AAO channel) helps align OMS pore orientation axially along the AAO channel. Therefore, complete filling and axial alignment requires deposition of colloidal particles, which is aided by the electric field. This packing of particles helps explain the morphological changes seen in Figure 3 and why ordered pore orientations are only apparent when 5 V is applied (Figures 1e,f and 2). When the electrophoretic deposition is stopped and the sol con-

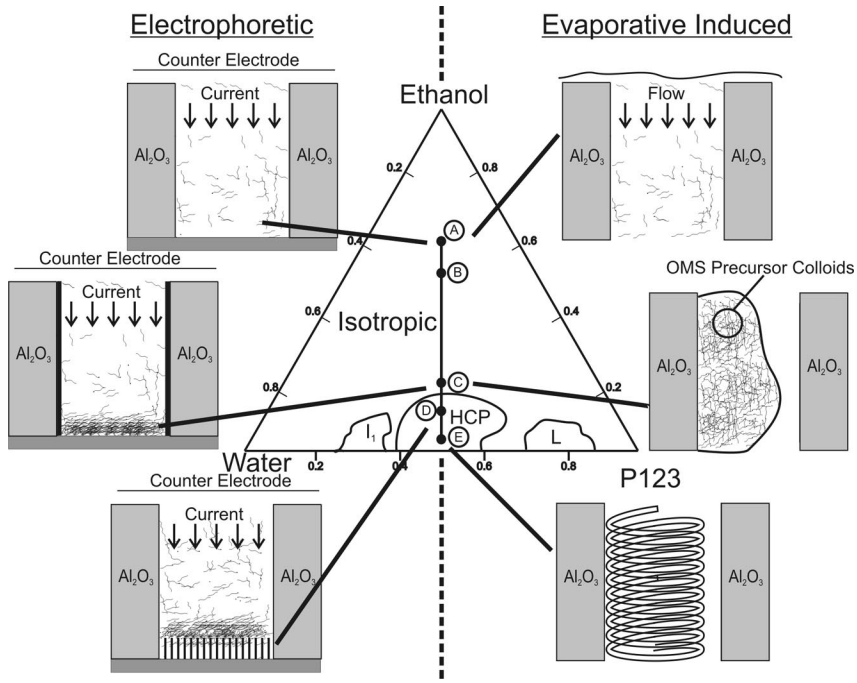

Figure 6. Water−P123−ethanol ternary phase diagram showing the HCP (hexagonal close packed) region. Points A−D on the phase diagram indicate various stages of the formation mechanisms for both evaporative induced self-assembly and electrophoretic deposition of OMS in AAO templates. Note that the points A−D in the phase diagram only occur in the area of the pore where packing density has reached a critical value and OMS growth is occurring. The solution above this region is isotropic. Experimental data taken from Soni et al.[27]

centration in the channel remains outside the HCP region (point C), evaporation-induced self-assembly can still occur, yielding the structures and voids seen in Figure 3a−c.

Conclusion

The ability to obtain axially oriented structures of increasingly smaller diameters is a key challenge in porous templates. In addition, the development of these templates on substrates may be important to the fabrication of nanostructures on conductive electrodes or other functional devices. Electrophoretic deposition of mesoporous silica is an approach that may lead to complete filling of axially oriented ordered mesoporous silica within the pores of anodic alumina membranes. The electric field appears to help drive the system into the HCP region of the phase diagram and orient the pores along the AAO channel.

Acknowledgment. Acknowledgment is made to the Donors of the American Chemical Society Petroleum Research Fund and UF Seed Fund for partial support of this research.

Supporting Information Available: Additional HRTEM images of OMS hierarchical nanostructures obtained at 0.3, 2.3, and 5 V and varying deposition times. This information is available free of charge via the Internet at http://pubs.acs.org.

CM803083S